The expression of aquaporins 1 and 5 in rat lung after thoracic irradiation

Cheng-Ying SUN[1], Yu-Xia ZHAO[1,*], Wen ZHONG[1], Da-Wei LIU[1], Yan-Zhi CHEN[1],
Li-Li QIN[1], Lu BAI[2] and Dan LIU[1]

[1]Department of Radiation Oncology, The Fourth Affiliated Hospital of China Medical University, No. 4 Chongshan Road, Huanggu District, Shenyang 110032, China
[2]Department of Radiation Oncology, The First Affiliated Hospital of China Medical University, No. 155 Nanjing Street, Heping District, Shenyang 110001, China
*Corresponding author. Department of Radiation Oncology, The Fourth Affiliated Hospital of China Medical University, No. 4 Chongshan Road, Huanggu District, Shenyang 110032, China. Tel: +86-138-0499-4607, +86-136-5418-6946; Fax: +86-024-6225-5001; Email: zyx_yd@163.com, 2448356540@qq.com

Radiation-induced lung toxicity (RILT), leading to radiation pneumonia or fibrosis, is a primary problem of radiation therapy. The pathogenesis of RILT remains unclear. In this study, we used a rat model of RILT to examine the expression of aquaporins (AQPs) after radiation injury. Sprague Dawley rats were given a single dose of 17 Gy (dose rate of 3.0 Gy/min) of X-irradiation to the thorax. Rats that survived acute pneumonitis (at 1–4 weeks) were evaluated weekly for the expression of AQP1 and AQP5 in the lung by immunohistochemical and reverse transcription polymerase chain reaction (RT-PCR) analyses. Immunohistochemical analysis showed that AQP1 protein was expressed in the capillary endothelium, and its level was significantly decreased after irradiation. AQP5 protein was expressed in the alveolar epithelium, and its level was increased between Days 7 and 14 after irradiation but decreased at Day 28, compared with the sham group. The RT-PCR results were consistent with the immunohistochemical analysis results. In summary, this study provides the first report of AQP1 and AQP5 expression in a model of radiation-induced pulmonary inflammation and edema. Decreased levels of AQP1 and AQP5 after irradiation suggest that these proteins play a role in the pathogenesis of RILT.

Keywords: radiation-induced lung toxicity; AQP1; AQP5

INTRODUCTION

Radiation therapy is one of the most important treatments for thoracic tumors. However, radiation-induced lung toxicity (RILT), leading to acute pneumonitis or fibrosis, has been reported, with an incidence rate of from 5–24% [1, 2]. The pathogenesis of RILT involves many factors such as dose, volume and cytokines [3].

After irradiation, early histopathological findings show diffuse alveolar damage [4]. This includes edema of the alveolar walls due to increased vascular permeability and exudation of proteins [5]. A number of pathological conditions (such as congestive heart failure, respiratory distress syndrome, and pulmonary edema resulting from injury or infection) can affect the lung and are characterized by disrupted fluid transport, which is related to aquaporins (AQPs) [6–8]. AQPs are a family of water-selective channels that are expressed in many tissues and function to increase plasma membrane water permeability and promote rapid fluid movement [9]. Four AQPs are expressed in the lung: AQP1 in the peribronchiolar and alveolar endothelia as well as in the visceral pleura; AQP3 in the trachea; AQP4 in airway epithelia and in the trachea; and AQP5 at the apical membrane of type I alveolar epithelial cells [10–12]. Decreased AQP1 and AQP5 levels have been reported in the mouse lung after acute adenoviral infection [8]. In addition, deletion of AQP1 in rats led to a 10-fold decrease in osmotically driven water transport between the airspace and capillary compartments, and a greater decrease in transcapillary water permeability [13]. Furthermore, AQP5 expression in cultured lung endothelial cells was decreased 2-fold at the mRNA level and 10-fold at the protein level after tumor necrosis factor-α (TNF-α) treatment.

It has been proposed that AQP1 and AQP5 may play important roles in the physiology and pathology of the lung [14]. We hypothesized that the expression of AQP1 and AQP5 in the lung is regulated by inflammation and edema. In this study, we analyzed the expression of AQP1 and AQP5 in the context of pulmonary inflammation and edema resulting from irradiation. To the best of our knowledge, this is the first report of the downregulation of AQP1 and AQP5 expression in a model of pulmonary edema after irradiation.

MATERIALS AND METHODS

Animals and irradiation
A total of 21 Sprague Dawley male rats (weighing ~210 ± 10 g, 6–8 weeks old, CMU Animal center, China) were used in this study. Rats were caged in groups of five or less, and all were fed with animal chow and water. All rats were acclimatized for at least 7 d before the initiation of experiments. Then, the rats were allocated to control (6 rats) and irradiation groups (15 rats). The animals were anesthetized with an intraperitoneal injection of 10% chloralic hydras (0.3 ml/100 g body weight), placed on the treatment table in the prone position, and a single dose of 17 Gy of radiation was delivered to both lungs at a dose rate of 3 Gy/min using a 6-MV X-ray linear accelerator (Varian 23EX, Palo Alto, CA, USA). The field was tested and verified by an electronic portal imaging device (EPID), with a source-to-skin distance of 100 cm. Control animals were treated with sham irradiation to both lungs. After irradiation, the rats were returned to the animal facility and given routine care. All the experiments were performed following the Institutional Guide for the Care and Use of Laboratory Animals.

Sample preparation
Sprague Dawley rats were sacrificed by intraperitoneal injection of 10% chloralic hydras (0.3 ml/100 g, Yangzhou Aoxin, China) at 7, 14 and 28 d after irradiation. At each timepoint, five rats in the irradiation group were killed. After locating the trachea and lungs by incision of the thoracic cage, the superior lobe of the right lung was removed to measure the wet weight, then desiccated in an oven (at 70°C for 24 h) to measure the dry weight, and the lung wet-to-dry weight ratio was calculated. The middle and inferior lobes of the right lung were kept at −80°C. The left lung was fixed in 10% neutral formalin buffer for 48 h, dehydrated, and wax embedded.

Immunohistochemical analysis
Paraffin-embedded lungs were sliced as 4-μm sections and stained with hematoxylin and eosin (H&E) for morphological analysis. For immunohistochemical staining, the sections were incubated with AQP1 and AQP5 antibodies (1:100, Abcam, USA). In the negative control, the antibody was replaced with phosphate-buffered saline. The staining

intensity in the lung tissue was measured with the Metanlorph/Evolution Mp5.0/BX51 US/JP image analysis system.

Reverse transcription polymerase chain reaction
Total RNA was extracted from the lung tissues with a total RNA purification kit (TaKaRa, Japan) and dissolved in 25 μl of diethylpyrocarbonate-treated water. The RNA concentration and quantity were determined using a spectrophotometer (DU-640; Beckman, USA), and 2 μg of the total RNA was used to synthesize single strand cDNA following the instructions of the reverse transcription polymerase chain reaction (RT-PCR) kit (TaKaRa, Japan). cDNA was amplified by PCR with primers specific for AQP1, AQP5 and GAPDH: AQP1 fwd-5CCA TGA CCC TCT TCG TCT TCA, rev-5TAG TCA ATG GCC AGC AGG TG; AQP5 fwd-5TGT GCT CCC TTG CCT TCT TC, rev-5TGG CCC AGT GTG ACA GAC AA; and GAPDH fwd-5GAAGGTCGGAGTC AACGGAT, rev-5CCTGGA AGATGG TGATGGG. The sequences of the primers were designed using Primer 5.0 software, and their specificity was confirmed by BLAST queries. The amplification was performed at 94°C for 3 min for predenaturation, 94°C for 30 s for denaturation, 59.7°C for 30 s for annealing, and 72°C for 45 s for extension for a total of 33 cycles, followed by a final extension for 7 min. PCR products (5 μl) were subjected to 1.5% agarose gel electrophoresis (Bio-Rad, USA) and the images were scanned by a Multi Genius Bioimaging System (Bio-Rad, USA) to calculate the ratio of the integrated optical densities for each product. The relative quantity of mRNA was calculated based on the opital densities with GAPDH (Abcam, USA) as the internal control.

Statistical analysis
The results were expressed as means ± standard errors and analyzed using the unpaired Student's t-test with equal variance. The analysis of variance of data was performed by using SPSS 13.0 statistical software. A difference with a *P*-value <0.05 was considered significant.

RESULTS

Histological analysis of the lung after irradiation
The early histopathological findings on Days 7 and 14 after irradiation showed a little intra-alveolar edema due to increased vascular permeability and exudation of proteins into the alveolar space. The alveolar space was integrated, the pulmonary capillaries were expanded, and hyperemia was present with some inflammatory cell infiltration (Fig. 1B–C). Increased inflammatory cell infiltration was observed on Day 28 after irradiation, consistent with pulmonary edema, vessel thrombosis, and intra-alveolar hemorrhage. Diffuse inflammatory cell infiltration was detected in broad areas of the

lung parenchyma (Fig. 1D). The severity of lung damage was variable between rats.

To quantitatively assess pulmonary edema after irradiation, the lung wet-to-dry weight ratios were determined. The lung wet-to-dry weight ratios from rats after irradiation were significantly increased both on Day 14 (119.16%, $n = 5$, $P < 0.05$) and on Day 28 (126.4%, $n = 5$, $P < 0.01$) after irradiation, compared with unirradiated rats ($n = 6$) (Table 1). The lung wet-to-dry weight ratio in rats on Day 7

after irradiation was slightly greater than in unirradiated rats, and the ratio in rats on Day 28 after irradiation was slightly greater than that on Day 14 after irradiation, but the differences did not reach statistical significance ($P > 0.05$).

Immunohistochemical analysis of AQP1 and AQP5 in the lung after irradiation

AQP1 has previously been shown to localize to the pulmonary vascular endothelium throughout the parenchyma of the lung and the surrounding vessels [11]. Although the localization of AQP1 staining remained unchanged in irradiated and sham-irradiated lungs (Fig. 2), AQP1 staining in irradiated lungs was weakened after irradiation (red or black arrow) on Days 7, 14 and 28 compared with sham-irradiated rats ($P = 0.000$, Table 2). The decrease in AQP1 staining was observed throughout the lungs and was not localized to regions of intense inflammation. Meanwhile, AQP5 staining was localized to the alveolar regions of the lung in sham-irradiated as well as in irradiated rats (Fig. 3). Compared with sham-irradiated rats, increased AQP5 staining was observed in rats treated with irradiation for 7 d and 14 d ($P = 0.01$), but
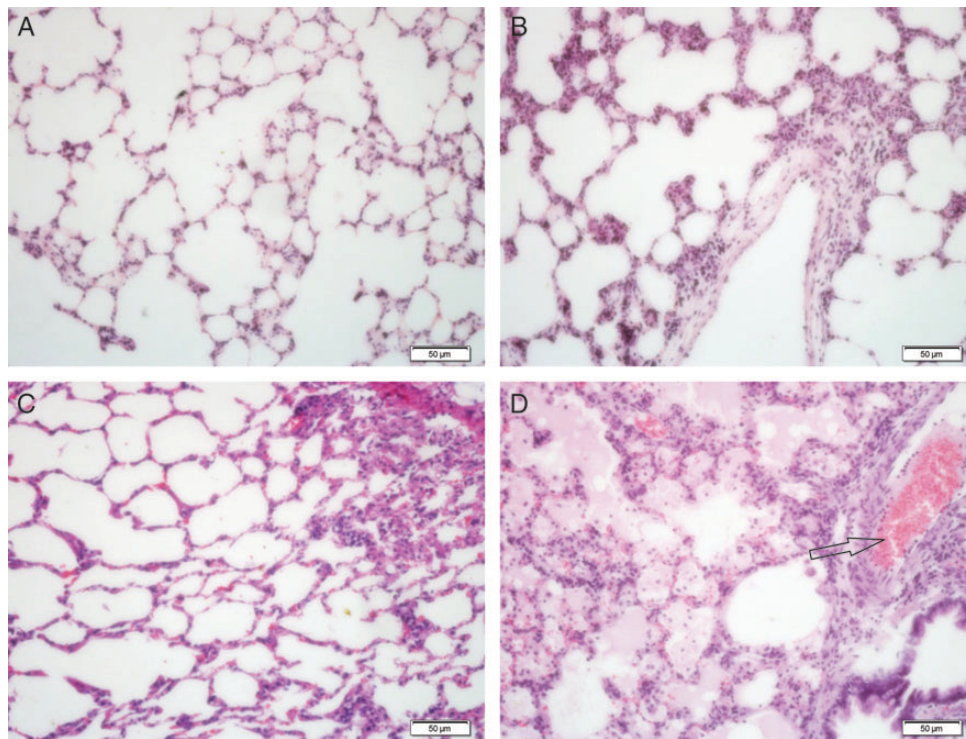
Table 1. Lung wet-to-dry weight ratios in different groups

Treatment	n	Wet-to-dry weight ratio
control	6	4.5018 ± 0.3631
RT 7 d	5	4.5238 ± 0.3522
RT 14 d	5	$5.3598 \pm 0.2936*$
RT 28 d	5	$5.6896 \pm 0.7860**$

RT = radiation treatment, *$P < 0.05$ vs control, **$P < 0.01$ vs control.

Fig. 1. Pulmonary histology after irradiation. Lung sections from a sham-irradiated rat (**A**) and rats 7 d (**B**), 14 d (**C**), and 28 d (**D**) after irradiation of 17 Gy were stained with H&E. On Days 7 and 14 after irradiation, intra-alveolar edema was obvious due to increased vascular permeability and exudation of proteins into the alveolar space. The alveolar space was integrated, pulmonary capillaries were expanded, and hyperemia was present with some inflammatory cell infiltration (B, C). Enlarged inflammatory cell infiltration was observed on Day 28 after irradiation, consistent with pulmonary edema, vessel thrombosis (arrows), and intra-alveolar hemorrhage. Diffuse inflammatory cell infiltration was detected in broad areas of the lung parenchyma (D). Scale bar: 50 μm.
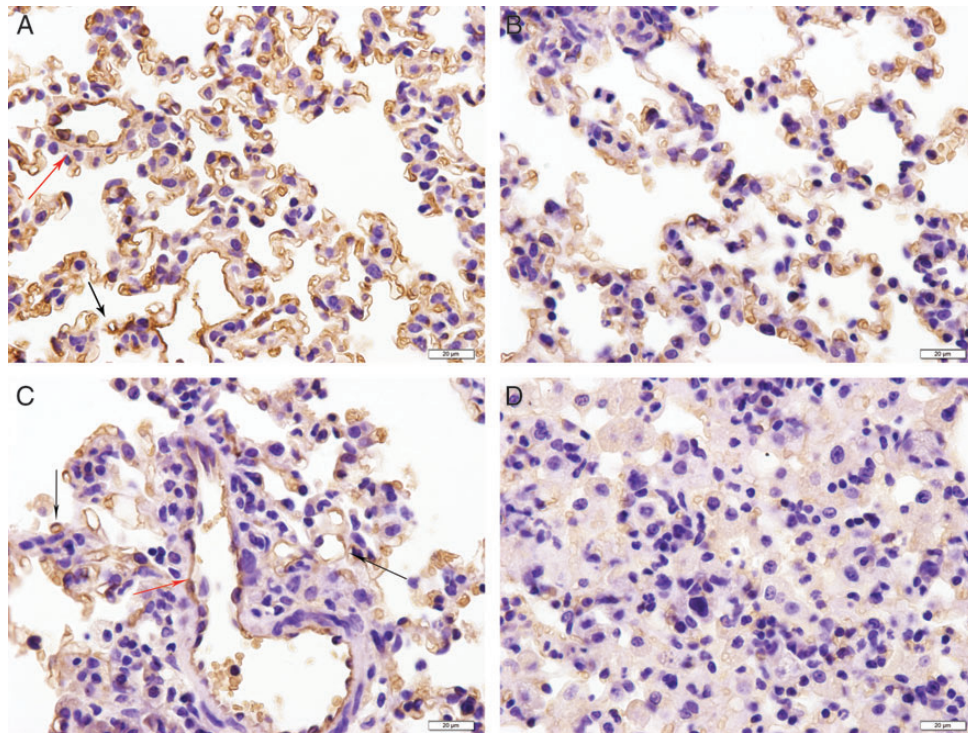
Fig. 2. Immunohistochemical staining of AQP1 in pulmonary vascular endothelial cells (PVECs) (red arrow) and capillary endothelial cells (black arrow) in irradiated lung tissue (17 Gy). (**A**) Control group. (**B**) 7 d postirradiation. (**C**) 14 d postirradiation. (**D**) 28 d postirradiation. Scale bar: 20 μm.

Table 2. IOD of AQP1 and AQP5 based on immunohistochemical staining

Treatment	AQP1	AQP5
control	741.3 ± 83.04	99.55 ± 10.05
RT 7 d	145.15 ± 20.13*	233.93 ± 29.42*
RT 14 d	229.64 ± 30.02*	131.56 ± 18.73**
RT 28 d	117.90 ± 20.42*	54.66 ± 8.03*

RT = radiation treatment, IOD = average integrated optical density, $*P = 0.000$ vs control, $**P = 0.01$ vs control.

AQP5 staining was decreased on Day 28 (Fig. 3A–D, Table 2). AQP5 staining in the lungs after irradiation was observed throughout the lung parenchyma, regardless of inflammatory cell infiltration.

Expression of AQP1 and AQP5 mRNA in the lung after irradiation

To determine whether the changes in AQP1 and AQP5 staining are due to changes in mRNA levels, RT-PCR was performed. AQP1 mRNA was expressed at low levels in the normal lung, but the AQP1 mRNA level was decreased within 28 d of irradiation compared with the sham-irradiation group. Densitometric analysis revealed that the AQP1

mRNA level was decreased to 61.77% at 7 d after irradiation, to 28.43% at 14 d after irradiation, and to 24.03% at 28 d after irradiation, compared with sham-irradiated animals (Fig. 4). In normal lung tissue, the expression of AQP5 mRNA was at a low level. Following thoracic irradiation, the AQP5 mRNA level in lung tissue was significantly increased on Day 7 to 147.62% ($P < 0.05$) of that in sham-irradiated animals; subsequently, the AQP5 mRNA level declined to basal levels ($P = 0.316$). Furthermore, the AQP5 mRNA level on Day 28 was decreased notably compared with the sham-irradiation group (Fig. 4).

DISCUSSION

In this study, we performed a detailed analysis of temporal expression of AQP1 and AQP5 in the lung tissue of rats after thoracic irradiation with defined doses. According to our preliminary test and previous studies [15–18], we chose a dose of 17 Gy to be delivered to both lungs because this dose resulted in obvious changes of the lungs for 28 d after irradiation. For the first time, the results of this study provide evidence of a clear time-dependent decrease in AQP1 and a fluctuation of AQP5 expression following irradiation exposure. In addition, the time-dependent expression of AQP1 mRNA and AQP5 mRNA correlated with immunohistochemical staining of AQP1 and AQP5 in the corresponding lung tissue.
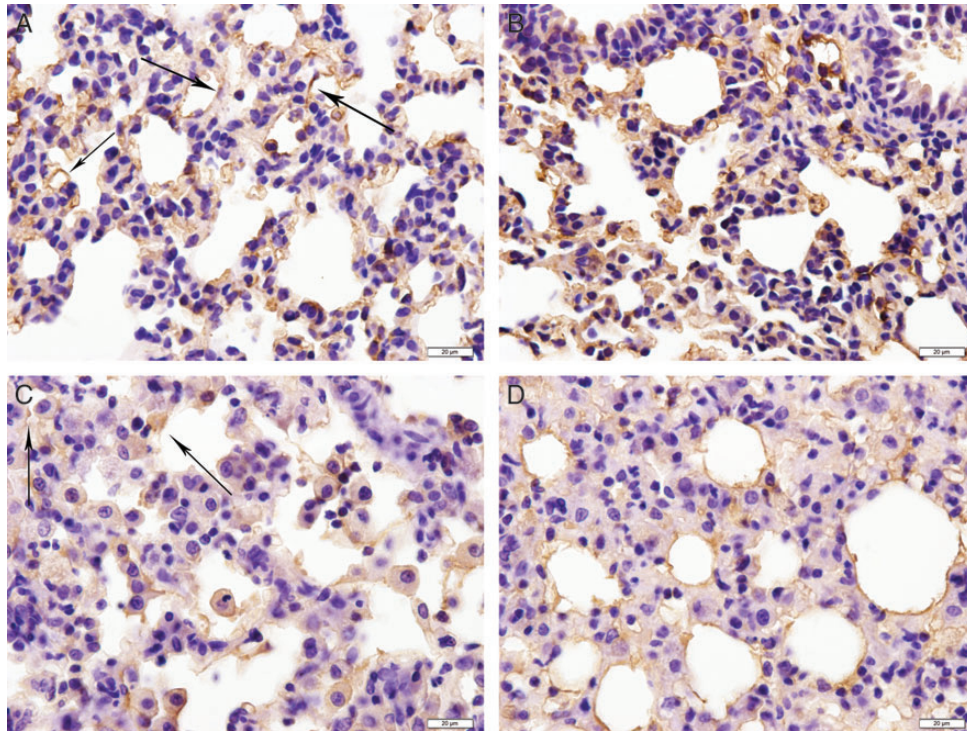
Fig. 3. Immunohistochemical staining of AQP5 in type I pneumocytes (marked by black arrows) in irradiated lung tissue (17 Gy). (**A**) Control group. (**B**) 7 d postirradiation. (**C**) 14 d postirradiation. (**D**) 28 d postirradiation. Scale bar: 20 μm.

Radiation-induced lung injury is characterized by the following histopathological features: (i) capillary congestion with thrombi; (ii) alveolar filling with protein-rich fluid, alveolar cell debris, macrophages, neutrophils and lymphocytes; and (iii) alveolar wall-thickening infiltrated by neutrophils and lymphocytes [19]. Based on these pathological changes, we successfully established an animal model of acute radiation-induced lung injury. A feature of radiation-induced lung injury is pulmonary edema, which represents a pathophysiological manifestation of fluid dysregulation. In our study, pulmonary edema was detected by histopathology and the wet-to-dry weight ratio of rat lungs on Days 7, 14 and 28 after irradiation. The early histopathological finding on Days 7 and 14 after irradiation was a little intra-alveolar edema due to increased vascular permeability and exudation of proteins into the alveolar space. The alveolar space was integrated, the pulmonary capillary was expanded, and hyperemia was present with some inflammatory cell infiltration. Enlarged inflammatory cell infiltration was observed 4 weeks after irradiation together with pulmonary edema, vessel thrombosis, and intra-alveolar hemorrhage. Diffuse inflammatory cell infiltration was detected in broad areas of the lung parenchyma. These findings are consistent with a previous report that the early histopathological finding after radiation is described as diffuse alveolar damage [4]. This includes edema of the alveolar walls due to increased vascular permeability and exudation of proteins into the alveolar space [5]. Vessel thrombosis may also occur, with focal necrosis and subsequent organization. In addition, intra-alveolar hemorrhage may occur. Infiltration with inflammatory cells is evident and, at least in experimental models, subsides rapidly within days [20]. Our results showed that the lung wet-to-dry weight ratios on Days 14 and 28 after irradiation were significantly increased compared with that of sham-irradiated rats. These histological findings and the increase in wet-to-dry weights are consistent with the presence of pulmonary edema in rats after irradiation.

The expression of lung AQP1 mRNA was significantly decreased in the context of pulmonary inflammation and edema resulting from irradiation. AQP1 mRNA expression was decreased in the lungs on Days 7, 14 and 28 after irradiation, and the decrease was the least on Day 28, indicating that the reduction in AQP1 expression is coincident with the increased inflammatory response. Likewise, immunohistochemical analysis of AQP1 demonstrated a reduction in AQP1 throughout the lungs of rats on Day 28 after irradiation. AQP1 staining was decreased but still detectable in highly inflamed regions of the lung, such as the peribronchial and perivascular regions. The presence of AQP1 in microvascular endothelia and some pneumocytes has been reported
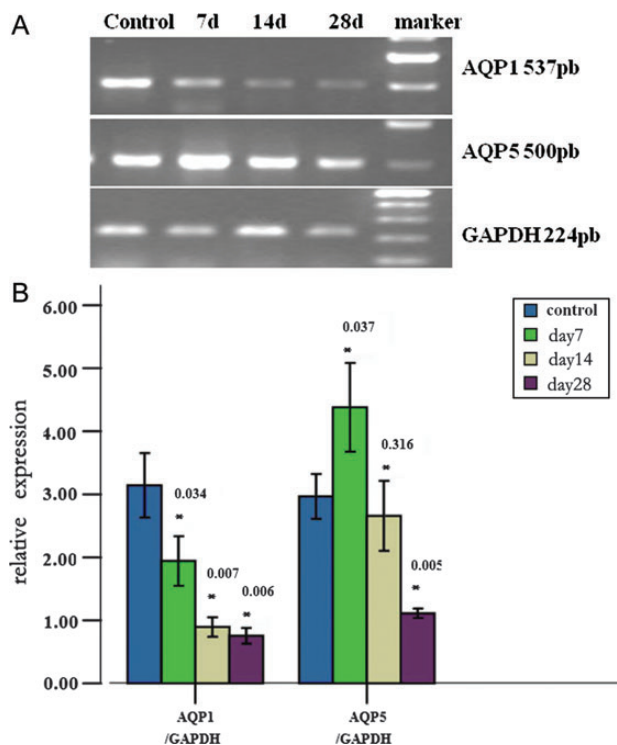
Fig. 4. AQP1 and AQP5 mRNA expression levels after irradiation. The mRNA levels of AQP1 and AQP5 in the lung tissues were evaluated by RT-PCR (**A**). AQP levels were normalized with the housekeeping gene GAPDH and expressed as levels relative to the control groups (**B**). The AQP1 mRNA level decreased in response to radiation-induced lung damage. The AQP5 mRNA level significantly fluctuated. *p-value vs control.

previously [21–23]. Early radiation-induced lung damage leads to direct endothelial damage and vasodilatation, as well as extravasation of proteins that enter the intra-alveolar space [24, 25]. In the present study, we observed a sustained decrease in AQP1 immunoreactivity and mRNA expression, which correlated with the overall degree of injury. Evidence of pulmonary edema was generally increased in the lungs of rats at 28 d after irradiation compared with the lungs of rats at 7 and 14 d after irradiation. Collectively, our results indicate that AQP1 is involved in the pathogenesis of radiation-induced lung damage.

Celine *et al.* noted decreased expression of AQP5 in the lungs of mice after a single 12-Gy dose or a fractionated 30-Gy dose at 14 weeks, and a time-dependent decrease after a fractionated 24-Gy dose from 1 month to 5 months [26]. In our study, the expression of lung AQP5 mRNA fluctuated in the context of pulmonary inflammation and edema resulting from irradiation. AQP5 mRNA expression and immunoreactivity were significantly increased in the lungs of rats 7 d after irradiation and subsequently appeared to return to normal levels 14 d after irradiation. AQP5 expression on Day 28 was decreased notably compared with the sham-irradiation

group. Taken together, these data indicate that downregulation of AQP5 results in abnormal lung fluid metabolism after irradiation and that AQP5 may play an important role in lung fluid clearance.

CONCLUSION

In conclusion, we demonstrated that radiation-induced pulmonary inflamation and edema in rats were associatiated with a marked reduction in the expression of AQP1 and significant fluctuation in the expression of AQP5. The predominant localization of AQP1 in endothelial cells and AQP5 in epithelial cells suggest the involvement of these two proteins in the pathogenesis of radiation-induced pulmonary injury. Further investigation will be necessary to clarify the detailed role of AQPs in radiation-induced lung damage. An improved understanding of the underlying mechanisms of radiation-induced lung injury may lead to modulatory intervention at the molecular level to control the fibrotic process. Molecularly targeted treatments have been used to prevent, mitigate or treat radiation-induced lung injury [27]. In addition, AQP1 gene transfer has been shown to correct radiation-induced salivary hypofunction in head and neck cancers [28]. Therefore, further studies should be performed to explore the potential of aquaporin gene transfer to treat radiation-induced lung injury.

FUNDING

REFERENCES

1. Kong FM, Ten Haken RK, Schipper MJ *et al*. High-dose radiation improved local tumor control and overall survival in patients with inoperable/unresectable non-small-cell lung cancer: long-term results of a radiation dose escalation study. *Int J Radiat Oncol Biol Phys* 2005;**63**:324–33.

2. Rubin P, Johnston CJ, Williams JP *et al*. A perpetual cascade of cytokines postirradiation leads to pulmonary fibrosis. *Int J Radiat Oncol Biol Phys* 1995;**33**:99–109.

3. Novakova-Jiresova A, Van Gameren MM, Coppes RP *et al*. Transforming growth factor-beta plasma dynamics and postirradiation lung injury in lung cancer patients. *Radiother Oncol* 2004;**71**:183–9.

4. Rosai J. Acute pulmonary injury interstitial pneumonia. In: Rosia J (ed.). *Ackerman's Surgical Pathology*, 8th edn. St Louis, MO: Mosby, 1996, 358–9.

5. Gross NJ. Experimental radiation pneumonitis. IV. Leakage of circulatory proteins onto the alveolar surface. *J Lab Clin Med* 1980;**95**:19–31.

6. Ma T, Fukuda N, Song Y *et al*. Lung fluid transport in aquaporin-5 knockout mice. *J Clin Invest* 2000;**105**:93–100.

7. Li ER, King LS. Induction of aquaporin-1 by bacterial infection. *Am J Respir Crit Care Med* 2002;**165**:A291.

8. Towne JE, Harrod KS, Krane CM *et al*. Decreased expression of aquaporin (AQP)1 and AQP5 in mouse lung after acute viral infection. *Am J Respir Cell Mol Biol* 2000;**22**:34–44.

9. King LS, Agre P. Pathophysiology of the aquaporin water channels. *Annu Rev Physiol* 1996;**58**:619–48.

10. Dobbs LG, Gonzalez R, Matthay MA *et al*. Highly water-permeable type I alveolar epithelial cells confer high water permeability between the airspace and vasculature in rat lung. *Proc Natl Acad Sci U S A* 1998;**95**:2991–6.

11. Effros RM, Darin C, Jacobs ER *et al*. Water transport and the distribution of aquaporin-1 in pulmonary air spaces. *J Appl Physiol* 1997;**83**:1002–16.

12. Nielsen S, King LS, Christensen BM *et al*. Aquaporins in complex tissues. II. Subcellular distribution in respiratory and glandular tissues of rat. *Am J Physiol* 1997;**273**:C1549–61.

13. Bai C, Fukuda N, Song Y *et al*. Lung fluid transport in aquaporin-1 and aquaporin-4 knockout mice. *J Clin Invest* 1999;**103**:555–61.

14. Song Y, Fukuda N, Bai C *et al*. Role of aquaporins in alveolar fluid clearance in neonatal and adult lung, and in oedema formation following acute lung injury: studies in transgenic aquaporin null mice. *J Physiol* 2000;**525**:771–9.

15. Liu CJ, Ha XQ, Jiang JJ *et al*. Keratinocyte growth factor (KGF) gene therapy mediated by an attenuated form of *Salmonella typhimurium* ameliorates radiation induced pulmonary injury in rats. *J Radiat Res* 2011;**52**:176–84.

16. Rube CE, Uthe D, Schmid KW *et al*. Dose-dependent induction of transforming growth factor beta (TGF-beta) in the lung tissue of fibrosis-prone mice after thoracic irradiation. *Int J Radiat Oncol Biol Phys* 2000;**47**:1033–42.

17. Kma L, Gao F, Fish BL *et al*. Angiotensin converting enzyme inhibitors mitigate collagen synthesis induced by a single dose of radiation to the whole thorax. *J Radiat Res* 2012;**53**:10–7.

18. Park KJ, Oh YT, Kil WJ *et al*. Bronchoalveolar lavage findings of radiation induced lung damage in rats. *J Radiat Res* 2009;**50**:177–82.

19. Rosiello RA, Merrill WW. Radiation-induced lung injury. *Clin Chest Med* 1990;**11**:65–71.

20. Abdollahi A, Li M, Ping G *et al*. Inhibition of platelet-derived growth factor signaling attenuates pulmonary fibrosis. *J Exp Med* 2005;**201**:925–35.

21. Nielsen S, Smith BL, Christensen EI *et al*. Distribution of the aquaporin CHIP in secretory and resorptive epithelia and capillary endothelia. *Proc Natl Acad Sci U S A* 1993;**90**:7275–9.

22. Folkesson HG, Matthay MA, Hasegawa H *et al*. Transcellular water transport in lung alveolar epithelium through mercury-sensitive water channels. *Proc Natl Acad Sci U S A* 1994;**91**: 4970–4.

23. King LS, Nielsen S, Agre P. Aquaporins in complex tissues. I. Developmental patterns in respiratory and glandular tissues of rat. *Am J Physiol* 1997;**273**:C1541–8.

24. Tsoutsou PG, Koukourakis MI. Radiation pneumonitis and fibrosis: mechanisms underlying its pathogenesis and implications for future research. *Int J Radiat Oncol Biol Phys* 2006;**66**:1281–93.

25. Travis EL, Harley RA, Fenn JO *et al*. Pathologic changes in the lung following single and multi-fraction irradiation. *Int J Radiat Oncol Biol Phys* 1977;**2**:475–90.

26. Almeida C, Nagarajan D, Tian J *et al*. The role of alveolar epithelium in radiation-induced lung injury. *PLOS One* 2013;**8**:e53628.

27. Komaki R, Liao Z, Cox JD. *Radioprotectors and Chemoprotectors in the Management of Lung Cancer. Advances in Radiation Oncology in Lung Cancer.* Springer, 2011, 223–45.

28. Baum BJ, Zheng C, Cotrim AP *et al*. Aquaporin-1 gene transfer to correct radiation-induced salivary hypofunction. *Handb Exp Pharmacol* 2009;**190**:403–18.